JOURNAL OF MATERIALS PROCESSING TECHNOLOGY 209 (2009) 1122–1128

journal homepage: www.elsevier.com/locate/jmatprotec

# Properties of $CO_2$ laser-welded butt joints of dissimilar magnesium alloys

*Pawel Kolodziejczak*[a,*], *Wojciech Kalita*[b]

[a] *Department of Production Engineering, Warsaw University of Technology, Narbutta 85, 02-524 Warszawa, Poland*
[b] *Institute of Fundamental Technological Research, Polish Academy of Sciences, Swietokrzyska 21, 00-049 Warszawa, Poland*

ARTICLE INFO

*Article history:*
Received 24 August 2007
Received in revised form
6 March 2008
Accepted 14 March 2008

*Keywords:*
Laser welding
Magnesium alloys
Microstructures
Mechanical properties
Corrosion resistance

ABSTRACT

The paper presents results of keyhole laser beam welding of dissimilar magnesium alloys that have been carried out with the $CO_2$ laser of maximum power of 2.5 kW. The workpieces of die-cast alloys AZ91 and AM50 with thicknesses of 4.5 mm have been butt-welded with helium used as a shielding gas. With the chosen flow rate of helium shielding and the focal position set on the metal surface the nearly parallel fusion zones boundaries were obtained. The analysis of microstructures of the joints, measurements of hardness distribution and the elemental distribution in the weld cross-sections permitted to find the changes due to heating in the fusion zones and recrystallization. The static tensile strength tests and the three point bending tests have allowed to determine the mechanical properties of the joints. The corrosion resistance tests performed by the electrochemical method on samples of as-cast materials and samples with the welds of similar and dissimilar alloys have not displayed the differences in the corrosion resistance. However, the microscopic observations of surfaces of welded samples have shown the influence of the joints on corrosion development.



## 1. Introduction

Increasing interest of automotive and aeronautic industries in magnesium alloys is mainly due to their much lower density with respect to traditional materials like steel and aluminum alloys.

The recent progress in the development of new casting techniques improved mechanical properties, machinability and corrosion resistance of magnesium alloys (Friedrich and Schumann, 2001; Mordike and Ebert, 2001). With properties of new magnesium alloys comparable with traditional materials it led to their applications as die-casting auto parts: gearboxes, valve covers, wheels, clutch housings, and brake pedal brackets (Longworth, 2001). The wider use of magnesium alloys in industrial applications may come with the dependable methods of components joining. Although such welding techniques like TIG and MIG are in use for many years their disadvantages (large fusion and heat affected zones, high shrinkage and deformations, defects such as cracks and porosity) gave rise to increased interest in laser welding method. Research papers published in last few years presented results obtained with different lasers: $CO_2$, Nd:YAG and diode lasers. Some investigations revealed difficulties concerned with post-welding defects such as porosity, cracks, and magnesium evaporation and undesirable changes in mechanical and other properties. The state of art in laser welding of magnesium alloys is provided in quite recent extensive review by Cao et al. (2006). It may be noticed that most results reported in the field of properties of laser-welded joints are concerned with the microstructure of welds and post-welding defects for par-

* *Corresponding author*. Tel.: +48 22 234 8759; fax: +48 22 849 9434.
E-mail address: pkolodzi@wip.pw.edu.pl (P. Kolodziejczak).
0924-0136/$ – see front matter © 2008 Elsevier B.V. All rights reserved.
doi:10.1016/j.jmatprotec.2008.03.072

ticular alloys. Relatively few investigations were carried out to determine the mechanical properties of joints like tensile strength and, especially, resistance to transverse loads. There is a lack of research of corrosion resistance of laser-welded joints: the fact surprising in situation when the microstructure of fusion zone significantly differs from the base material.

In case of laser welding of AM50 and AZ91 alloys the investigations of Lehner and Reinhart (1999) have shown that lower power level and slower speed led to better weld quality, while in Marya and Edwards (2001) study it was found that high beam powers reduce both ripples and crowning. Researching the influence of focal position Lehner and Reinhart (1999) found that better results (penetration depth and aspect ratio) are obtained for the focal position below the workpiece surface (for thicknesses of 3 and 5 mm) while Weisheit et al. (1998) achieved good results with on-surface focal position for thicknesses less than 5 mm. Marya and Edwards (2001) also found that these two magnesium alloys responded differently to $CO_2$ laser welding: much greater penetration depth could be reached in AM50 than AZ91 alloy welded under similar conditions. Important conclusion derived from experiments of Weisheit et al. (1998) was that the joints of die-cast alloys showed extremely high level of porosity.

In the present study the investigation of properties of $CO_2$ laser-welded butt joints of similar and dissimilar alloys comprised the study of microstructures, evaluation of profiles of hardness and elemental distributions and static tensile and bending tests. Also, the new results of corrosion resistance tests are reported as continuation of previous investigations (Kalita et al., 2004; Kwiatkowski et al., 2005).

## 2. Methodology

The materials studied are die-cast magnesium alloys AZ91 and AM50 with the chemical composition given in Table 1. The samples to be welded were machined from as-cast bars to the strips with thickness of 4.5 mm, width of 50 mm and welding edge length of 100 mm.

Prior to welding the surfaces of the edges were mechanically cleaned with abrasive paper and degreased with acetone. The butt-welding has been performed with $CO_2$ laser of maximum power 2.5 kW. The beam with the mode close to $TEM_{10}$ was focused to the diameter of 0.25 mm by the ZnSe lens of 5 in. No filler metal has been used. The samples were mechanically clamped. The welding tests have been performed in the range of laser power from 1.8 to 2.5 kW and with the scanning velocity from 2.5 to 5 m/min. For the topside shielding the helium was provided from the nozzle with orifice diameter of 4 mm coaxially with the laser beam. The flow rate of helium was changed in the range from 10 to 40 l/min. From the evaluation of macrostructures of the joints (as the main criterion) it was found that optimal conditions, when the fusion zones have nearly parallel boundaries and no cracks and porosity appeared in the welds, have been as follows: laser power has been set at 2 kW, the welding rate at 0.067 m/s (4 m/min) and the flow rate of helium was $2.5 \times 10^{-4}$ m$^3$/s (15 l/min). After evaluation of the influence of the focal point position (with respect to material surface) on the shape of fusion zone, the beam focal position has been set on the upper surface of plates. The bottom surfaces of samples were shielded by the blow of argon. In these conditions six joints of similar alloys and six of dissimilar alloys were made.

**Table 1 – Chemical composition of welded alloys**

| Alloy | Alloying elements (% wt) | | |
|---|---|---|---|
| | Al | Zn | Mn |
| AM50 | 5 | <0.2 | 0.3 |
| AZ91 | 9 | 0.7 | 0.17 |

The microstructures and the hardness profiles have been evaluated on the cross-sections perpendicular to the direction of beam scanning on six samples for each kind of joint. Also, the microstructures were observed on the cross-sections done parallelly to the facing surface along the seam. In order to find any changes due to the action of laser beam (e.g. evaporation of material and thermocapillary convection) the analysis of elemental distribution of basic elements has been performed with X-ray microprobe. The mechanical properties of the joints have been examined by the tests on the Instron stand for static tensile strength and the transverse bending. After the fracture of workpieces the SEM images of weld fractures were obtained to compare with fractures of the parental material. The comparative corrosion resistance tests have been performed by electrochemical method (cyclic voltammetry) followed by microscopic examinations.

## 3. Results

The main characteristic of the joints obtained with the keyhole laser welding is a very narrow fusion zone with nearly parallel boundaries. For the butt-welded samples of 4.5 mm in thickness the fusion zones have widths less than 1.3 mm (Fig. 1). With the welding rate of 4 m/min the time of irradiation is very short and solidification is fast so the fusion zones are characterized by significant grain refinement.

The sharp transitions from the base metal to the fusion zone may indicate that there is no heat-affected zone. On the microscopic enlargements it may be observed that the distinguished direction of recrystallization at the fusion boundary is only several grains wide (Fig. 2).

The parental materials, used in experiments, were of high quality and contained no pores and after welding in the chosen conditions the fusion zones have been practically free of pores. In some cases the oscillations of the fusion zones along the seam were observed (Fig. 3). The value of frequency of oscillations (less than 100 Hz) suggests that observed oscillations are not associated with oscillations of the keyhole (usually of order of some kHz as it has been shown by Szymanski et al., 2001).

For the determination of changes in the chemical composition of material caused by the influence of beam action the measurements of elemental distributions have been performed by means of X-ray microprobe. Line content distributions are presented in Fig. 4 for the AZ91 joint in Fig. 5 for AM50 joint and in Fig. 6 for the joint of dissimilar alloys. It may

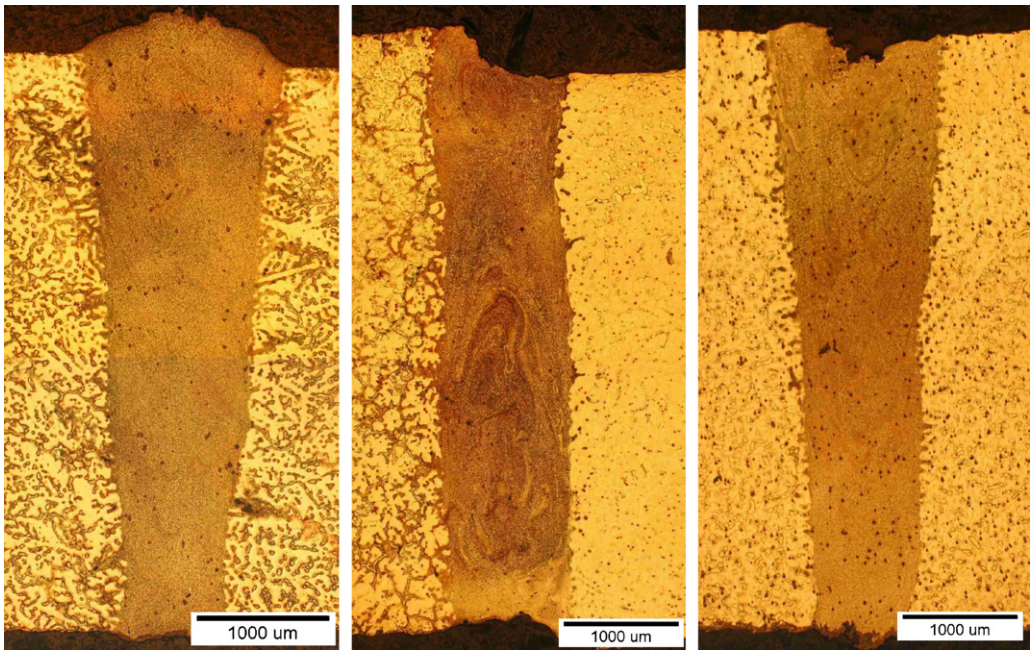


**Fig. 1 – Macrosections of butt-welded joints: AZ91 + AZ91, AZ91 + AM50, AM50 + AM50.**

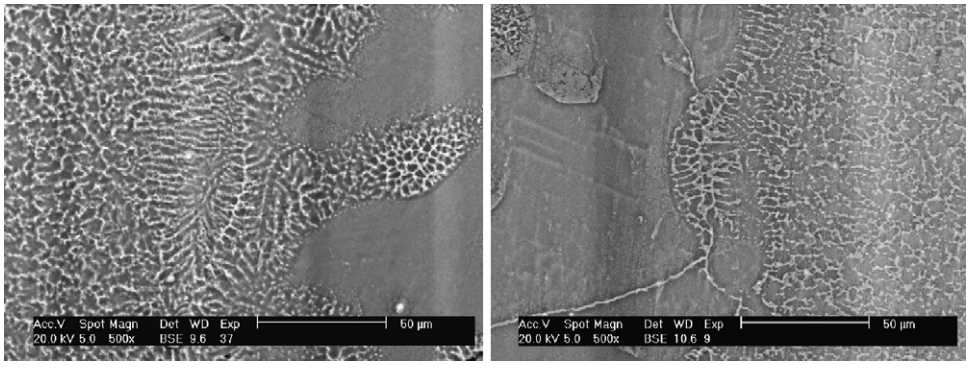


**Fig. 2 – SEM images of microstructures at fusion zone boundaries: a. AZ91 joint, b. AM50 joint.**


**Fig. 3 – Oscillations of the fusion zone in the cross section parallel to the facing surface (AZ91 joint, cross section made at 1.5 mm from the face surface).**

be observed that in the fusion zones the elemental concentration profiles, especially aluminum, have been much uniform than outside welds.

Nonhomogeneous as-cast material contained many large precipitations and after laser beam melting the fine-grained structure is obtained. It was also found that due to the very low boiling point of magnesium (~1100 °C) in comparison with that of aluminum (~2300 °C), the percentage share of aluminum in the joints (especially in AZ91 weld) has been slightly increased by evaporation of magnesium.

The measurements of hardness distributions in the cross-sections of welds of similar alloys (perpendicular to the direction of welding) have shown significant increase of hardness in the fusion zones in comparison with the base material, particularly for the AZ91 joint. From the microhardness profiles presented in Fig. 7 it is seen that for AZ91 joint the

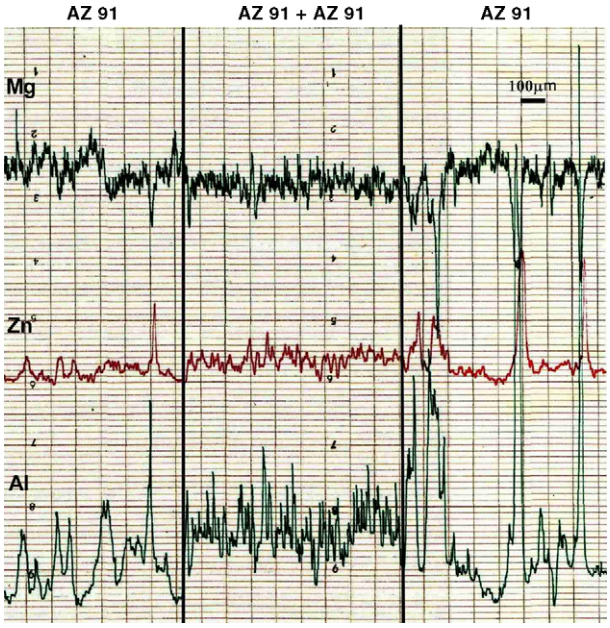


**Fig. 4 – Linear elemental distributions across the weld of AZ91 joint.**

maximum value is over 100 HV (base metal: 70 HV) and for AM50 joint about 70 HV (for the base metal: 60 HV). These results may be associated not only with the high grain refinement in the welds but also with appearance of intermetallic compounds. Some decrease in hardness at the fusion boundaries may be observed. This effect can indicate that the heat-affected zones that have not been observed on microstructures of the joints are present at the fusion boundaries. In result the softening in these regions decreased the hardness. For the microhardness of the joints of dissimilar alloys (Fig. 8) no such effects were found.

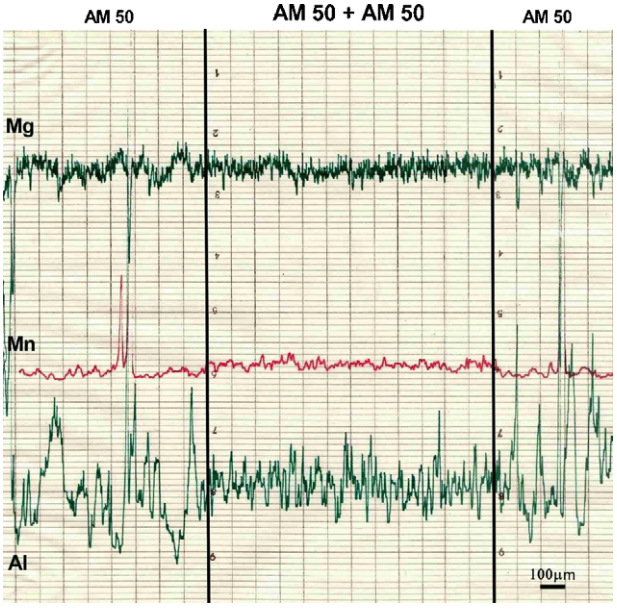


**Fig. 5 – Linear elemental distributions across the weld of AM50 joint.**

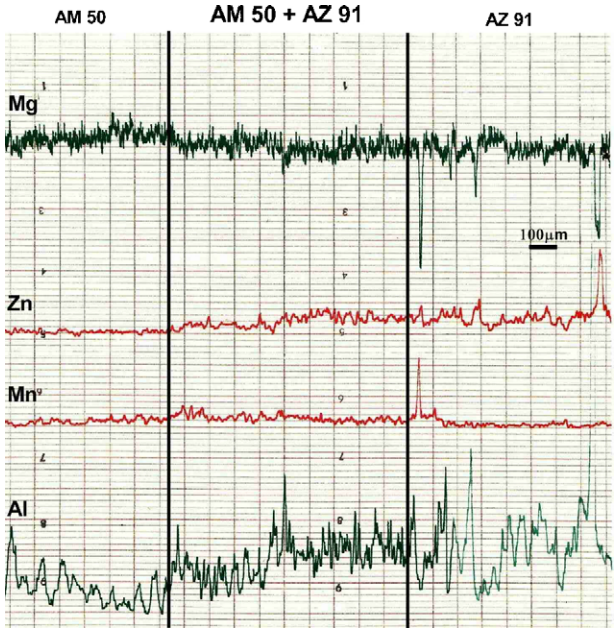


**Fig. 6 – Linear elemental distributions across the weld of AZ91 + AM50 joint.**

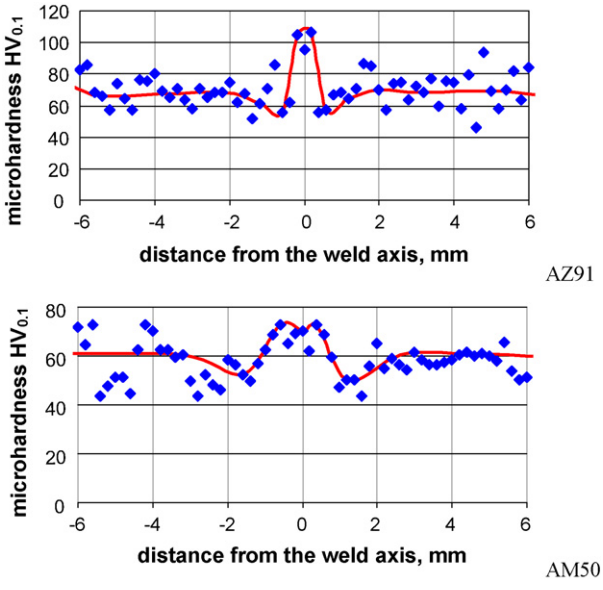


**Fig. 7 – Hardness distributions in the cross sections of the joint of similar alloys.**

The comparative static tensile strength tests for the samples made of base metal and the samples with joints have been performed on the Instron stand. The samples with joints were prepared in such a way that the weld axis has been located at the center of the sample. The stress vs. strain curves for joints of similar alloys and base metal samples (6 samples for each kind of joint and 6 for base metal) are presented in Fig. 9. In all tests the fractures of the welded samples occurred beyond the fusion zone: from 1.5 to 6 mm from the boundary of weld. That result may be associated with nonhomogenity of as-cast base material in comparison to the microstructure in the weld. As it could be expected the samples with joints have smaller elon-

**Table 2 – Results of uncertainty analysis for base metal samples and the joints for confidence interval equal to 95 % ($s^2$ – sample variance)**

| | Base metal AZ91 | Joint AZ91 + AZ91 | Base metal AM50 | Joint AM50 + AM50 | Joint AZ91 + AM50 |
|---|---|---|---|---|---|
| $S^2$ | 17.90 | 14.20 | 15.50 | 14.77 | 18.40 |
| Tensile stresses | 134.5 ± 4,44 | 114.5 ± 3,95 | 175.5 ± 4.13 | 145.7 ± 4.03 | 145.0 ± 4.50 |

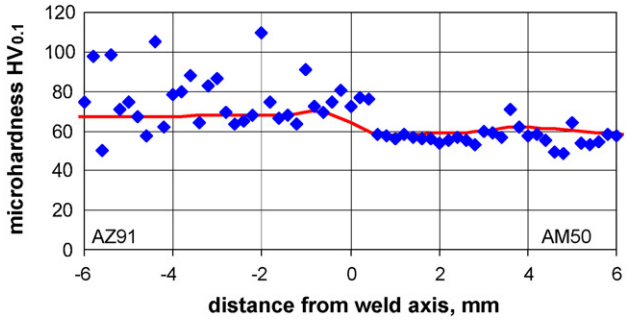


**Fig. 8 – Hardness distributions in the cross section of the AZ91+AM50 joint.**

gation at fracture than the parental materials however there are differences for tensile strengths: for AM50 joint the stress at fracture is lower and for AZ91 joint is higher than those for base metal samples. The results of uncertainty analysis for base metal samples and the joints made by T-Student's test are given in Table 2.

Since the fracture in both cases occurred far from the fusion zones the SEM images did not display differences between the

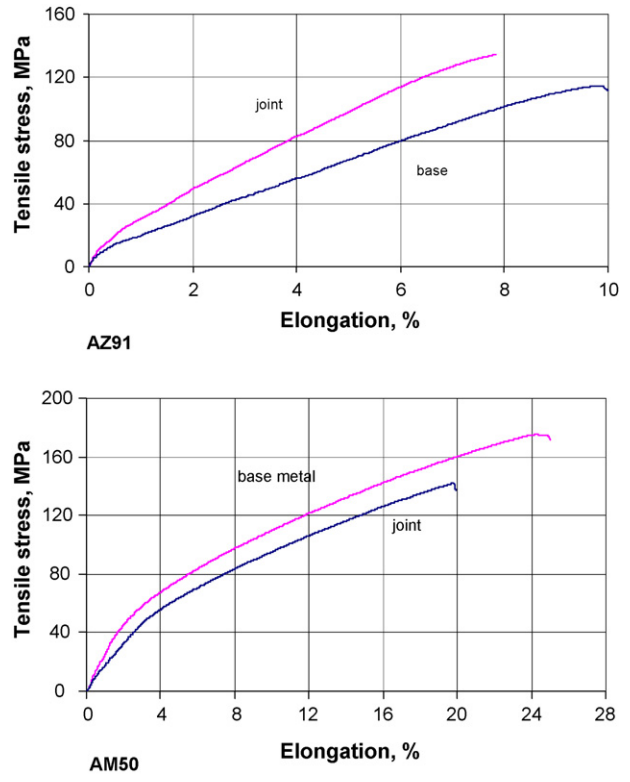


**Fig. 9 – Tensile stress – strain curves for base metal samples and samples with the joints of similar alloys.**

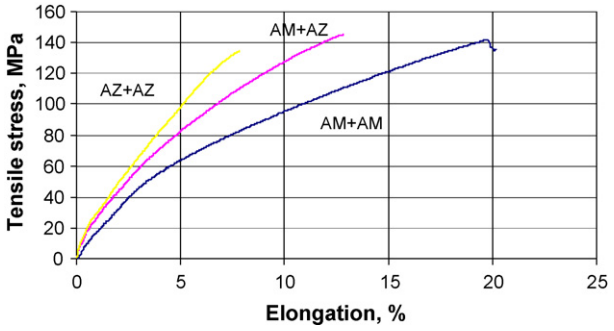


**Fig. 10 – Tensile stress – strain curves for samples with the joints of similar and dissimilar alloys.**

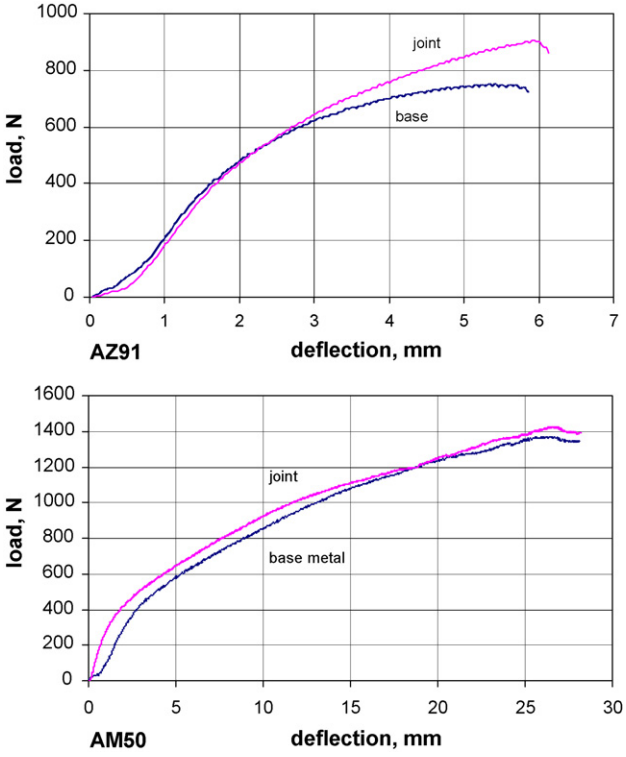


**Fig. 11 – Load vs. deflection curves for joints of similar alloys and base metal samples.**

base metal samples and the samples with the joints. In both cases the images present the ductile behaviour of material. The yield strength for the AZ91 alloy is practically unnoticed while for AM50 alloy may be estimated at about 50 MPa. For the joints of AZ91 + AM50 the workpieces broke at the AZ91 side, also far from the fusion zone. The comparison of stress–strain curves for all joints is given in Fig. 10. According to anticipations the elongation at fracture for dissimilar joints has the value between those of the joints of AZ91 alloy and AM50 alloy.

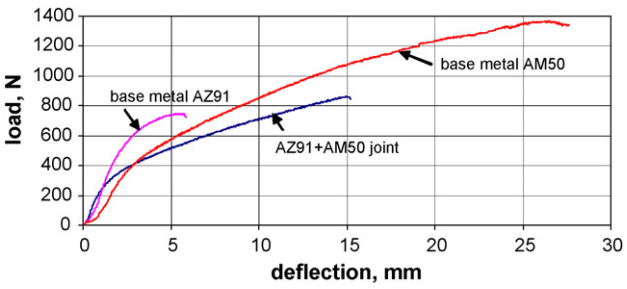


**Fig. 12 – Load vs. deflection curves for joint of dissimilar alloys and samples of parental metals.**

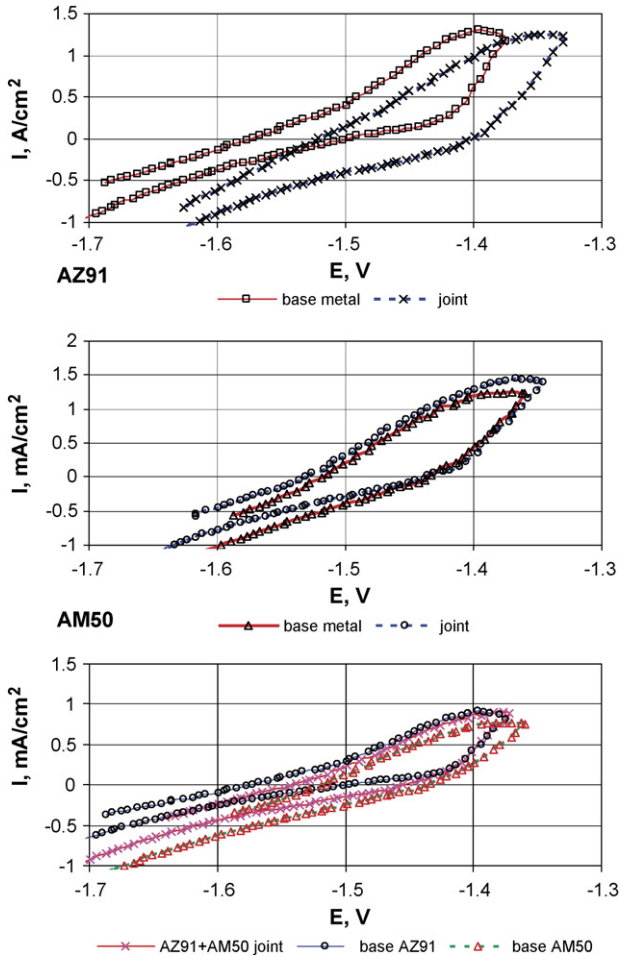


**Fig. 13 – Polarisation curves for base metal samples and samples with joints.**

The static bending tests were carried out on the three-point bend stand with support rollers' spacing of 70 mm and the rollers' diameter of 30 mm. Six samples made of parental metal and six with the joints for each alloy have been tested with the weld across the width of a sample and the face of weld in tension. The load versus deflection curves for joints of similar alloys are presented in Fig. 11. It may be observed that for AZ91 alloy the base metal sample and the sample with joint have been broken at nearly the same value of deflection (6 mm) but the peak load for base metal is considerably lower than for the joint. For much more ductile alloy AM50 the bending

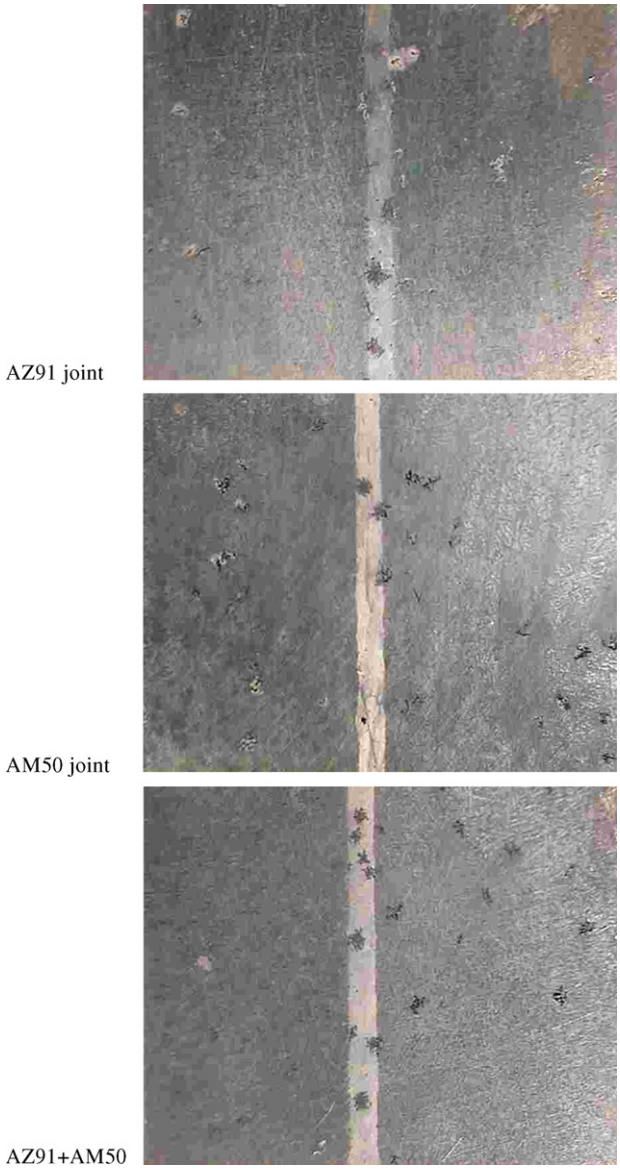


**Fig. 14 – The surfaces of the joints and the surroundings after corrosion tests.**

up to 160° did not bring to fracture and there were no differences between curves for base metal samples and samples with joints. The comparison of bending curves for samples of parental metals and the joint of dissimilar alloys is presented in Fig. 12.

The comparative corrosion resistance tests of samples made of parental material and the samples with joints have been performed by electrochemical method. Current–potential curves were recorded after 1 h of immersion in aerated 9% NaCl water solution while attaining the stable open-circuit potential. Measurements were carried out in three electrode cell (working electrode—sample with the surface area of 2 $cm^2$; counter electrode—platinum gauze; reference—saturated calomel electrode) and were realised by means of Solartron Electrochemical Interface 1287 with a potential sweep 1 mV/s from −100 to 300 mV versus OCP. The polarisation curves, (Fig. 13) ascertained limited corro-

sion resistance of base metal samples as well as the samples with the joints. However, these measurements show insignificant differences between curves for the base metal and the joints and also for the values of potential of catastrophic corrosion. These values may be assessed between −1.40 and −1.44 V.

The microscopic and SEM observations of the surfaces of the joints and surrounding areas, performed after corrosion tests, provided more informations about the influence of the weld on corrosion resistance (Fig. 14). While the corrosion pits in base metal samples are disposed uniformly and randomly, the pits on the samples with AZ91 joint are concentrated in the area of the weld. This area contained smaller amount of magnesium than the surroundings and plays the role of anodic electrode. For the samples with AM50 joint the corrosion pits are localized randomly on the surface, however their size in the area of weld is greater than in base metal surface. For the joints of dissimilar alloys the corrosion process gives different results than in joints of similar alloys. The corrosion pits are localized only on the AM50 side and in the fusion zone that is effect of more anodic potential of these areas than that of the AZ91 side.

## 4. Conclusions

The following remarks can be made concerning the properties of the $CO_2$ laser butt-welded joints of magnesium alloys AZ91 and AM50 with thicknesses of 4.5 mm:

(1) Under chosen conditions of welding (laser power: 2 kW, welding rate: 0.067 m/s, helium shielding, the focal position of the beam on the material surface) the joints have very narrow fusion zones with nearly parallel boundaries and they are practically free of pores and cracks.
(2) Due to high welding rate and fast recrystallization the fusion zones are characterized by very high grain refinement that resulted in increase of hardness in these regions in comparison with parental material. For the joints of similar alloys some decrease of hardness may be observed at the fusion zone boundaries. This effect can indicate that the heat-affected zones that have not been observed on microstructures of the joints are present at the fusion boundaries.
(3) The comparative static tensile strength tests for the samples made of base metal and the joints of similar alloys displayed smaller elongation at fracture of the joints however tensile strengths for AM50 joint at fracture is lower and for AZ91 is higher than those for base metal samples. For the joints of dissimilar alloys the workpieces broke at the AZ91 side, far from the fusion zone. According to anticipations the elongation at fracture for these joints has the value between those of the joints of AZ91 alloy and more ductile AM50 alloy.
(4) The static bending tests indicated that for AZ91 alloy the maximum load at fracture for the welded samples was higher than for the base material. The samples of AM50 alloy, characteristic of high plasticity, were bent up to 160° without fracture both for welded specimens as well as base material.
(5) The comparative corrosion resistance tests performed by electrochemical method have not shown differences in resistance between the base metal samples and the samples with joints. For both alloys the corrosion resistance is relatively low. However, the microscopic and SEM observations of sample surfaces after corrosion tests have shown that in the areas of weld the concentration of pits is higher than outside (AZ91 alloy) or the pits have grown faster than in the base material (AM50 alloy).

In conclusion, it is possible to affirm that the $CO_2$ laser welding of as-cast magnesium alloys is effective method to obtain the joints with mechanical properties comparable with the base material. However, the corrosion protection of joints is required.

## REFERENCES

Cao, X., Jahazi, M., Immarigeon, J.P., Wallace, W., 2006. A review of laser welding techniques for magnesium alloys. J. Mater. Process. Technol. 171, 188–204.
Friedrich, H., Schumann, S., 2001. Research for a “new age of magnesium” in the automotive industry. J. Mater. Process. Technol. 117, 276–281.
Kalita, W., Kolodziejczak, P., Kwiatkowski, L., Hoffman, J., 2004. Properties of the butt-welded joints of $CO_2$ laser welded Mg alloys. In: Geiger, M., Otto, A. (Eds.), Proceedings of the LANE. Meisenbach-Verlag Bamberg, Erlangen, Germany, vol. 1, pp. 317–328.
Kwiatkowski, L., Grobelny, M., Kalita, W., Kolodziejczak, P., 2005. Corrosion properties of the butt-welded joints of laser welded Mg alloys. Inzynieria Powierzchni 2A, 191–197.
Lehner, C., Reinhart, G., 1999. Welding of die-casted magnesium alloys for production. J. Laser Appl. 11 (5), 206–210.
Longworth, S.J.P., 2001. The bolting of magnesium components in car engines. A dissertation submitted for the degree of Master of Philosophy to the University of Cambridge.
Marya, M., Edwards, G.R., 2001. Factors controlling the magnesium weld morphology in deep penetration welding by a $CO_2$ laser. J. Mater. Eng. Perform. 10 (4), 435–443.
Mordike, B.L., Ebert, T., 2001. Magnesium. Properties – applications – potential. Mater. Sci. Eng. A302, 37–45.
Szymanski, Z., Hoffman, J., Kurzyna, J., 2001. Plasma plume oscillations during welding of thin metal sheets with cw $CO_2$ laser. J. Phys. D: Appl. Phys. 34, 189–199.
Weisheit, A., Galun, R., Mordike, B.L., 1998. $CO_2$ laser beam welding of magnesium-based alloys. Weld. Res. Suppl. 77 (4), 149–154.